Inorganic Chemistry
Article

Inorg. Chem. **2010**, *49*, 261–270 **261**
DOI: 10.1021/ic901956g

Heats of Formation of XeF_3^+, XeF_3^-, XeF_5^+, XeF_7^+, XeF_7^-, and XeF_8 from High Level Electronic Structure Calculations

Daniel J. Grant, Tsang-Hsiu Wang, and David A. Dixon*

Department of Chemistry, University of Alabama, Tuscaloosa, Alabama 35487-0336

Karl O. Christe

Loker Hydrocarbon Research Institute and Department of Chemistry, University of Southern California, University Park, Los Angeles, California 90089

Received October 4, 2009

Atomization energies at 0 K and heats of formation at 0 and 298 K are predicted for XeF_3^+, XeF_3^-, XeF_5^+, XeF_7^+, XeF_7^-, and XeF_8 from coupled cluster theory (CCSD(T)) calculations with effective core potential correlation-consistent basis sets for Xe and including correlation of the nearest core electrons. Additional corrections are included to achieve near chemical accuracy of ± 1 kcal/mol. Vibrational zero point energies were computed at the MP2 level of theory. Unlike the other neutral xenon fluorides, XeF_8 is predicted to be thermodynamically unstable with respect to loss of F_2 with the reaction calculated to be exothermic by 22.3 kcal/mol at 0 K. XeF_7^+ is also predicted to be thermodynamically unstable with respect to the loss of F_2 by 24.1 kcal/mol at 0 K. For XeF_3^+, XeF_5^+, XeF_3^-, XeF_5^-, and XeF_7^-, the reactions for loss of F_2 are endothermic by 14.8, 37.8, 38.2, 59.6, and 31.9 kcal/mol at 0 K, respectively. The F^+ affinities of Xe, XeF_2, XeF_4, and XeF_6 are predicted to be 165.1, 155.3, 172.7, and 132.5 kcal/mol, and the corresponding F^- affinities are 6.3, 19.9, 59.1, and 75.0 kcal/mol at 0 K, respectively.

Introduction

The first stable noble-gas compounds, the xenon fluorides, have been known[1,2] since the early 1960s beginning with the work of Bartlett.[3] The syntheses of XeF_2, XeF_4, XeF_6, and $XeOF_4$ were described within a year of the original discovery.[4−7] There is a continuing chemistry of xenon, and a substantial variety of xenon compounds have been synthesized and structurally characterized.[8,9] Xenon trifluoride radicals have recently been observed in a solid argon matrix on the basis of spectroscopic measurements.[10] We have recently performed extensive CCSD(T)/CBS (complete basis set) calculations on the rare gas xenon and krypton fluorides to predict their heats of formation and showed that the heats of formation need to be remeasured.[11,12] We showed that XeF_6 is fluxional because of the presence of a sterically active, free valence electron pair on Xe and that the structure is difficult to predict requiring the use of very large basis sets. At the CCSD(T)/CBS level and using an estimated geometry for the C_{3v} structure, the C_{3v} and O_h structures of XeF_6 have essentially the same energy, with the O_h structure only 0.19 kcal/mol below the C_{3v} one. However, the C_{3v} structure was predicted to become slightly lower in energy than the O_h one at the optimized C_{3v} geometry. We have previously reported on the fluoride affinities of a variety of compounds as the binding of F^- can be considered as a measure of the Lewis acidity.[13] We have also reported on the F^+ affinities, which

*To whom correspondence should be addressed. E-mail: dadixon@bama.ua.edu.

(1) Bartlett, N.; Sladky, F. O. The Chemistry of Krypton, Xenon and Radon. In *Comprehensive Inorganic Chemistry*; Bailar, J. C., Jr., Emeléus, H. J., Nyholm, R., Trotman-Dickenson, A. F., Eds.; Pergamon Press: Oxford, U.K., 1973; Vol. *1*, pp 213−330.
(2) Malm, J. G.; Selig, H.; Jortner, J.; Rice, S. A. *Chem. Rev.* **1965**, *65*, 199.
(3) (a) Bartlett, N. *Proc. Chem. Soc.* **1962**, 218. (b) Graham, L.; Gaudejus, O.; Jha, N. K.; Bartlett, N. *Coord. Chem. Rev.* **2000**, *197*, 321.
(4) Hoppe, R.; Dahne, W.; Mattauch, H.; Rodder, K. M. *Angew. Chem., Int. Ed. Engl.* **1962**, *1*, 599.
(5) Hoppe, R.; Dahne, W.; Mattauch, H.; Rodder, K. M. *Angew. Chem.* **1962**, *74*, 903.
(6) Classen, H. H.; Selig, H.; Malm, J. G. *J. Am. Chem. Soc.* **1962**, *84*, 3593.
(7) Malm, J. G.; Sheft, I.; Chernick, C. L. *J. Am. Chem. Soc.* **1963**, *85*, 110.
(8) Holloway, J. H.; Hope, E. G. *Adv. Inorg. Chem.* **1998**, *46*, 51–100.
(9) Whalen, J. M.; Schrobilgen, G. J. *Helium-Group Gases, Compounds*, 4th ed.; John Wiley and Sons, Inc.: New York, 1994; Vol. *13*, pp 38−53.
(10) Misochko, E. Y.; Akimov, A. V.; Belov, V. A.; Tyurin, D. A. *Inorg. Chem.*, **2009**, *48*, 8723.
(11) Dixon, D. A.; de Jong, W. A.; Peterson, K. A.; Christe, K. O.; Schrobilgen, G. J. *J. Am. Chem. Soc.* **2005**, *127*, 8627.
(12) Dixon, D. A.; Wang, T.-H.; Grant, D. J.; Peterson, K. A.; Christe, K. O. *Inorg. Chem.* **2007**, *46*, 10016.
(13) Christe, K. O.; Dixon, D. A.; McLemore, D.; Wilson, W. W.; Sheehy, J.; Boatz, J. A. *J. Fluorine Chem.* **2000**, *101*, 151. *Chem. Eng. News*, March 3, **2003**, pp 48−49.

© 2009 American Chemical Society
Published on Web 12/08/2009

provide a quantitative oxidizing strength scale for oxidative fluorinators.[14]

In our recent study of the heats of formation of the iodine fluorides employing a comparable CCSD(T)/CBS method, we found that it is very important to include the core electrons in the treatment of the correlation energy along with the appropriate weighted core valence basis sets and to extrapolate these quantities to the CBS limit to get chemical accuracy (±1 kcal/mol) in the total atomization energies.[15] We have extended our work on the xenon fluorides and have predicted the heats of formation for XeF_3^+, XeF_3^-, XeF_5^+, XeF_7^+, XeF_7^-, and XeF_8 at the CCSD(T)/CBS level using the new effective core potential/correlation consistent basis sets developed by Peterson and co-workers.[16] We also re-evaluated the heats of formation of XeF_2, XeF_4, XeF_5^-, and XeF_6 and have examined the energetics of XeF_3 and XeF_5 as well.

Computational Methods

We have been developing a composite approach[17] to the prediction of the thermodynamic properties of molecules based on molecular orbital theory using coupled cluster methods at the CCSD(T) level.[18−20] The standard aug-cc-pV*n*Z, with n = D − Q, basis sets were used for F.[21] A small core relativistic effective core potential (RECP) was used for Xe,[16] which subsumes the ($1s^2$, $2s^2$, $2p^6$, $3s^2$, $3p^6$, $3d^{10}$) orbital space into the 28-electron core, and a 26 electron space ($4s^2$, $4p^6$, $5s^2$, $4d^{10}$, and $5p^6$) with the electrons handled explicitly. We have previously shown that inclusion of the nearest core electrons in the valence electron correlation energy calculations for the iodine fluoride compounds was critical for the prediction of reliable energetics.[15] We included all 26 electrons outside the RECP core in our new xenon fluoride calculations with the aug-cc-pwCV*n*Z-PP basis sets[15,22] for D, T, and Q for Xe and aug-cc-pwCV*n*Z on F.[23] We abbreviate the combination of aug-cc-pwCV*n*Z on F and aug-cc-pwCV*n*Z-PP on Xe basis sets as awCV*n*Z. Calculations on Xe where only the $5s^2$ and $5p^6$ electrons are active in our valence correlation treatment are abbreviated by the shorthand notation of aV*n*Z to denote the combination of the aug-cc-pV*n*Z basis set on F and the aug-cc-pV*n*Z-PP basis set on Xe.[16,21] Only the spherical component subset (e.g., 5-term d functions, 7-term f functions, etc.) of the Cartesian polarization functions were used.

For the open shell calculations, we used the R/UCCSD(T) (restricted method for the starting Hartree−Fock wave function and then relaxed the spin restriction in the coupled cluster portion of the calculation) approach.[24−26] Our CBS estimates use a mixed exponential/Gaussian function of the form[27]

$$E(n) = E_{CBS} + Be^{-(n-1)} + Ce^{-(n-1)^2} \quad (1)$$

with n = 2 (awCVDZ), 3 (awCVTZ), 4 (awCVQZ) giving $E_{CBS}(DTQ)_{CV}$. The atomic spin−orbit correction for F is $\Delta E_{SO}(F)$ = 0.39 kcal/mol.[28] Another relativistic correction to the atomization energy accounts for molecular scalar relativistic effects, ΔE_{SR}, due to the F atoms. ΔE_{SR} was evaluated from the expectation values for the two dominant terms in the Breit−Pauli Hamiltonian (the mass-velocity and one-electron Darwin (MVD) corrections)[29] from configuration interaction singles and doubles (CISD) calculations with a VTZ basis set at the CCSD(T)/aVTZ geometry. We have shown that any "double counting" of the relativistic effect on Xe when applying a MVD correction to an energy, which already includes most of the relativistic effects via the RECP, is small.[11,15]

Geometries were optimized at the CCSD(T) level with the aVDZ and aVTZ basis sets where only the valence electrons are correlated with the aug-cc-pV*n*Z-PP basis set and RECP on Xe and the aV*n*Z basis set on F.[15,16,21] For the awCV*n*Z calculations, the geometries obtained with the aVDZ basis set were used in single point awCVDZ calculations and those with the aVTZ basis set in single point awCVTZ and awCVQZ calculations. For XeF_3^+ and XeF_3^-, the zero point energies (ΔE_{ZPE}) were calculated at the CCSD(T)/aVTZ level, for XeF_3 at the CCSD(T)/aVDZ level, and for the remaining molecules at the MP2/aVTZ//MP2/aVTZ level. For XeF_3^+, the ΔE_{ZPE} at the MP2/aVTZ level was calculated to be 3.96 kcal/mol, 0.1 kcal/mol higher than the CCSD(T)/aVTZ value. Thus, the ΔE_{ZPE} at the MP2/aVTZ level provides good estimate of the ZPE.

By combining our computed $\sum D_0$ values given by the following expression

$$\sum D_0 = \Delta E_{elec}(CBS) - \Delta E_{ZPE} + \Delta E_{SR} + \Delta E_{SO} \quad (2)$$

with the known[30] heats of formation at 0 K for the elements, $\Delta H_f^0(Xe)$ = 0 kcal/mol and $\Delta H_f^0(F)$ = 18.47 ± 0.07 kcal/mol, we can derive ΔH_f^0 values for the molecules under study. Heats of formation at 298 K were obtained by following the procedures outlined by Curtiss et al.[31] The calculated heats of formation at T = 298K for the ionic species were obtained with the ion convention (stationary electron convention).[30,32]

(14) Christe, K. O.; Dixon, D. A. *J. Am. Chem. Soc.* **1992**, *114*, 2978.
(15) Dixon, D. A.; Grant, D. J.; Peterson, K. A.; Christe, K. O.; Schrobilgen, G. J. *Inorg. Chem.* **2008**, *47*, 5485.
(16) (a) Peterson, K. A. *J. Chem. Phys.* **2003**, *119*, 11099. (b) Peterson, K. A.; Figgen, D.; Goll, E.; Stoll, H.; Dolg, M. *J. Chem. Phys.* **2003**, *119*, 11113.
(17) (a) Feller, D.; Dixon, D. A. *J. Phys. Chem. A* **2000**, *104*, 3048. (b) Feller, D.; Dixon, D. A. *J. Chem. Phys.* **2001**, *115*, 3484. (c) Dixon, D. A.; Feller, D.; Peterson, K. A. *J. Chem. Phys.* **2001**, *115*, 2576. (d) Feller, D.; Dixon, D. A. *J. Phys. Chem. A* **2003**, *107*, 9641. (e) Dixon, D. A.; Feller, D.; Christe, K. O.; Wilson, W. W.; Vij, A.; Vij, V.; Jenkins, H. D. B.; Olson, R. M.; Gordon, M. S. *J. Am. Chem. Soc.* **2004**, *126*, 834. (f) Dixon, D. A.; Gutowski, M. *J. Phys. Chem. A* **2005**, *109*, 5129. (g) Pollack, L.; Windus, T. L.; de Jong, W. A.; Dixon, D. A. *J. Phys. Chem. A* **2005**, *109*, 6934. (h) Feller, D.; Peterson, K. A.; Dixon, D. A. *J. Chem. Phys.* **2008**, *129*, 204015. (i) Ruscic, B.; Wagner, A. F.; Harding, L. B.; Asher, R. L.; Feller, D.; Dixon, D. A.; Peterson, K. A.; Song, Y.; Qian, X.; Ng, C.; Liu, J.; Chen, W.; Schwenke, D. W. *J. Phys. Chem. A* **2002**, *106*, 2727.
(18) Purvis, G. D., III; Bartlett, R. J. *J. Chem. Phys.* **1982**, *76*, 1910.
(19) Raghavachari, K.; Trucks, G. W.; Pople, J. A.; Head-Gordon, M. *Chem. Phys. Lett.* **1989**, *157*, 479.
(20) Watts, J. D.; Gauss, J.; Bartlett, R. J. *J. Chem. Phys.* **1993**, *98*, 8718.
(21) (a) Dunning, T. H., Jr. *J. Chem. Phys.* **1989**, *90*, 1007. (b) Kendall, R. A.; Dunning, T. H., Jr.; Harrison, R. J. *J. Chem. Phys.* **1992**, *96*, 6796.
(22) DeYonker, N. J.; Peterson, K. A.; Wilson, A. K. *J. Phys. Chem. A* **2007**, *111*, 11383.
(23) Peterson, K. A.; Dunning, T. H., Jr. *J. Chem. Phys.* **2002**, *117*, 10548.
(24) Rittby, M.; Bartlett, R. J. *J. Phys. Chem.* **1988**, *92*, 3033.
(25) Knowles, P. J.; Hampel, C.; Werner, H.-J. *J. Chem. Phys.* **1994**, *99*, 5219.
(26) Deegan, M. J. O.; Knowles, P. J. *Chem. Phys. Lett.* **1994**, *227*, 321.
(27) Peterson, K. A.; Woon, D. E.; Dunning, T. H., Jr. *J. Chem. Phys.* **1994**, *100*, 7410.
(28) Moore, C.E. *Atomic energy levels as derived from the analysis of optical spectra, Volume 1, H to V*; U.S. National Bureau of Standards Circular 467, U.S. Department of Commerce, National Technical Information Service, COM-72−50282: Washington, DC, 1949.
(29) Davidson, E. R.; Ishikawa, Y; Malli, G. L. *Chem. Phys. Lett.* **1981**, *84*, 226.
(30) Chase, M. W., Jr. NIST-JANAF Tables, 4th ed.; *J. Phys. Chem. Ref. Data*, Mono. 9, Suppl. 1, **1998**.
(31) Curtiss, L. A.; Raghavachari, K.; Redfern, P. C.; Pople, J. A. *J. Chem. Phys.* **1997**, *106*, 1063.
(32) Lias, S. G.; Bartmess, J. E.; Liebman, J. F.; Holmes, J. L.; Levin, R. D.; Mallard, W. G. *J. Phys. Chem. Ref. Data 17*, **1988**; Supplement 1. Gas Phase and Ion Chemistry.

All CCSD(T) calculations were performed with either the MOLPRO-2002[33] program system on a single processor of an SGI Origin computer or the DMC at the Alabama Supercomputer Center or with NWChem[34] and MOLPRO on the massively parallel HP Linux cluster in the Molecular Science Computing Facility in the William R. Wiley Environmental Molecular Sciences Laboratory. The MP2 calculations were done with the Gaussian program system.[35]

Results and Discussion

The calculated geometries are summarized in Figure 1 where they are compared to experiment.[36−39] The calculated frequencies are given in Table 1 where they are compared with the available experimental values. The frequencies were obtained at the MP2/aVTZ level as were the IR intensities. Raman intensities were obtained at the density functional theory level with the B3LYP exchange-correlation functional[40] and the aVTZ basis set. The frequencies are reported to aid in the experimental detection of unknown molecules. The total energies used in this study are given in Supporting Information (Tables SM-1 and SM-2).

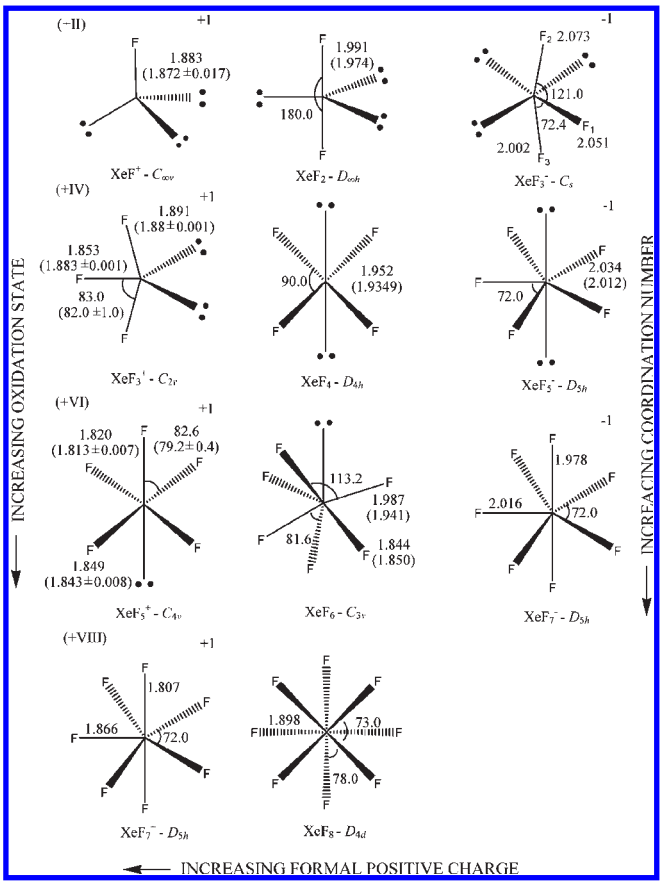

Figure 1. Calculated CCSD(T)/aVTZ and experimental geometry parameters, the latter in parentheses, of the xenon fluoride molecules and their ions (bond lengths in angstroms and bond angles in degrees). The calculated structures for XeF^+, XeF_2, XeF_4, XeF_5^-, and XeF_6 were taken from ref 11. Experimental geometries: XeF^+ (ref 41), XeF_2 (ref 36), XeF_3^+ (ref 42), XeF_4 (ref 37), XeF_5^+ (ref 43), XeF_5^- (ref 38), XeF_6 (C_{3v}) (ref 39), and XeF_7^- (C_{2v}, C_{3v}) (ref 46).

Geometries. We have previously predicted that the bond length in XeF^+ at the CCSD(T)/aVTZ level[11] is about 0.01 Å too long as compared to experiment,[41] so we expect our calculated CCSD(T)/aVTZ values to be long as compared to experiment by a comparable amount. The MP2/aVTZ value for $r(XeF^+)$ is calculated to be 0.005 Å too short compared to the experimental value.

The structure of XeF_3^+ is T-shaped with C_{2v} symmetry and is derived from a trigonal bipyramid with 2 lone pairs occupying the equatorial positions with a Xe in the +4 oxidation state. The calculated geometry is in good agreement with the experimental one from the crystal structure.[42] The calculated $Xe-F_e$ distance is about 0.03 Å too short as compared to experiment, and the $Xe-F_a$ distance is calculated to be 0.011 Å too long as compared to average experimental value.[42] The $Xe-F_a$ distance is slightly longer, and the $Xe-F_e$ distance is slightly shorter than $r(XeF^+)$.[11]

The neutral radical XeF_3 has a T-shaped structure with C_{2v} symmetry. The two identical Xe−F bond lengths are calculated to be 1.974 Å at the CCSD(T)/aVTZ level, slightly shorter by 0.019 Å than r(XeF) in XeF_2 of 1.993 Å

(33) Werner, H.-J.; Knowles, P. J. *MOLPRO a package of ab initio programs*, version 2002.6; Amos, R. D.; Bernhardsson, A.; Berning, A.; Celani, P.; Cooper, D. L.; Deegan, M. J. O.; Dobbyn, A. J.; Eckert, F.; Hampel, C.; Hetzer, G.; Knowles, P. J.; Korona, T.; Lindh, R.; Lloyd, A. W.; McNicholas, S. J.; Manby, F. R.; Meyer, W.; Mura, M. E.; Nicklass, A.; Palmieri, P.; Pitzer, R.; Rauhut, G., Schütz, M.; Schumann, U.; Stoll, H., Stone, A. J.; Tarroni, R.; Thorsteinsson, T.; Werner, H.-J.; Universität Stuttgart: Stuttgart, Germany; University of Birmingham: Birmingham, United Kingdom.

(34) (a) Apra, E.; Bylaska, E. J.; Jong, W. d.; Hackler, M. T.; Hirata, S.; Pollack, L.; Smith, D.; Straatsma, T. P.; Windus, T. L.; Harrison, R. J.; Nieplocha, J.; Tipparaju, V.; Kumar, M.; Brown, E.; Cisneros, G.; Dupuis, M.; Fann, G. I.; Fruchtl, H.; Garza, J.; Hirao, K.; Kendall, R.; Nichols, J. A.; Tsemekhman, K.; ; Valiev, M.; Wolinski, K.; Anchell, J.; Bernholdt, D.; Borowski, P.; Clark, T.; Clerc, D.; Dachsel, H.; Deegan, M.; Dyall, K.; Elwood, D.; ; Glendening, E.; Gutowski, M.; Hess, A.; Jaffe, J.; Johnson, B.; Ju, J.; Kobayashi, R.; ; Kutteh, R.; Lin, Z.; Littlefield, R.; Long, X.; Meng, B.; Nakajima, T.; ; Niu, S.; Rosing, M.; Sandrone, G.; Stave, M.; Taylor, H.; ; Thomas, G.; ; Lenthe, J. v.; Wong, A.; Zhang, Z. *NWChem*. William R. Wiley Environmental Molecular Sciences Laboratory, Pacific Northwest National Laboratory: Richland, WA, 2003.(b) Kendall, R. A.; Apra, E.; Bernholdt, D. E.; Bylaska, E. J.; Dupuis, M.; Fann, G. I.; Harrison, R. J.; Ju, J.; Nichols, J. A.; Nieplocha, J.; Straatsma, T. P.; Windus, T. L.; Wong, A. T. *Comput. Phys. Commun.* **2000**, *128*, 260.

(35) Frisch, M. J.; Trucks, G. W.; Schlegel, H. B.; Scuseria, G. E.; Robb, M. A.; Cheeseman, J. R.; Montgomery, Jr., J. A.; Vreven, T.; Kudin, K. N.; Burant, J. C.; Millam, J. M.; Iyengar, S. S.; Tomasi, J.; Barone, V.; Mennucci, B.; Cossi, M.; Scalmani, G.; Rega, N.; Petersson, G. A.; Nakatsuji, H.; Hada, M.; Ehara, M.; Toyota, K.; Fukuda, R.; Hasegawa, J.; Ishida, M.; Nakajima, T.; Honda, Y.; Kitao, O.; Nakai, H.; Klene, M.; Li, X.; Knox, J. E.; Hratchian, H. P.; Cross, J. B.; Bakken, V.; Adamo, C.; Jaramillo, J.; Gomperts, R.; Stratmann, R. E.; Yazyev, O.; Austin, A. J.; Cammi, R.; Pomelli, C.; Ochterski, J. W.; Ayala, P. Y.; Morokuma, K.; Voth, G. A.; Salvador, P.; Dannenberg, J. J.; Zakrzewski, V. G.; Dapprich, S.; Daniels, A. D.; Strain, M. C.; Farkas, O.; Malick, D. K.; Rabuck, A. D.; Raghavachari, K.; Foresman, J. B.; Ortiz, J. V.; Cui, Q.; Baboul, A. G.; Clifford, S.; Cioslowski, J.; Stefanov, B. B.; Liu, G.; Liashenko, A.; Piskorz, P.; Komaromi, I.; Martin, R. L.; Fox, D. J.; Keith, T.; Al-Laham, M. A.; Peng, C. Y.; Nanayakkara, A.; Challacombe, M.; Gill, P. M. W.; Johnson, B.; Chen, W.; Wong, M. W.; Gonzalez, C.; and Pople, J. A. *Gaussian 03*, Revision E.01; Gaussian, Inc.: Wallingford, CT, 2004.

(36) XeF_2 :Burger, H.; Kuna, R.; Ma, S.; Breidung, J.; Thiel, W. *J. Chem. Phys.* **1994**, *101*, 1.

(37) XeF_4: Burger, H.; Ma, S.; Breidung, J.; Thiel, W. *J. Chem. Phys.* **1995**, *104*, 4945.

(38) XeF_5^-: Christe, K. O.; Curtis, E. C.; Mercier, H. P.; Sanders, J. C. P.; Schrobilgen, G. J.; Dixon, D. A. *J. Am. Chem. Soc.* **1991**, *113*, 3351.

(39) XeF_6 (C_{3v}): Pitzer, K. S.; Bernstein, L. S. *J. Chem. Phys.* **1975**, *63*, 3849.

(40) (a) Becke, A. D. *J. Chem. Phys.* **1993**, *98*, 5648. (b) Lee, C.; Yang, W.; Parr, R. G. *Phys. Rev. B* **1988**, *37*, 785.

(41) Bartlett, N.; Gennis, M.; Gibler, D. D.; Morrell, B. K.; Zalkin, A. *Inorg. Chem.* **1973**, *12*, 1717.

(42) McKee, D. E.; Zalkin, A.; Bartlett, N. *Inorg. Chem.* **1973**, *8*, 1713.

Table 1. Calculated MP2/aVTZ Frequencies in cm^{-1} and Infrared and Raman Intensities at the DFT-B3LYP Level[a]

		MP2			B3LYP	
molecule	symmetry	frequency	expt.	*I* (IR)	frequency	*I* (Raman)
XeF^+ ($C_{\infty v}$)[b]	σ^+	680.2	621	8.3	696.7	11.6
XeF_3^+ (C_{2v})[c]	a_1	653.2	618	19.6	651.1	15.3
	a_1	608.4	582	0.5	597.3	30.1
	a_1	224.2		13.9	186.3	0.4
	b_1	207.7		11.5	220.7	0.0
	b_2	681.4	640	150.2	665.8	0.1
	b_2	326.3	358	6.0	308.0	2.3
XeF_3 (C_{2v})[d]	a_1	530.4/577.3	523	0.0	523.5	40.7
	a_1	216.8/201.8		15.8	247.8	20.2
	a_1	29.4/187.3		0.0	202.2	3.5
	b_1	217.6/207.0		14.3	226.7	0.0
	b_2	578.8/631.7	568	246.4	571.7	0.7
	b_2	9.5/87.5		0.0	86.6	6.0
XeF_3^- (C_s)	a′	512.1		228.1	432.8	2.1
	a′	457.4		99.8	393.4	25.3
	a′	233.5		10.2	249.1	6.7
	a′	220.4		113.6	238.2	6.9
	a′	89.6		65.8	87.7	1.9
	a″	202.3		20.9	176.2	0.0
XeF_5^+ (C_{4v})[e]	a_1	714.3	679	29.2	671.9	18.6
	a_1	655.7	625	0.9	627.7	30.5
	a_1	338.5	355	35.6	297.8	1.0
	b_1	288.4	300	0.0	274.9	2.6
	b_2	648.2	610	0.0	614.6	17.5
	b_2	218.8	261	0.0	189.3	0.1
	e	723.9	652	168.6	695.2	0.4
	e	377.3	410	10.4	346.6	3.2
	e	209.7	218	3.3	203.9	0.3
XeF_5 (C_{4v})	a_1	559.3		0.0	558.3	94.6
	a_1	293.9		34.5	287.2	7.4
	b_1	216.3		0.0	221.5	5.9
	b_2	523.7		0.0	520.2	26.8
	b_2	168.7		0.0	167.3	0.0
	b_2	6.3		0.0	242.8	15.4
	e	604.2		261.9	593.0	0.8
	e	159.1		1.8	164.3	0.0
	e	4.9		0.0	87.8	10.5
XeF_7^+ (D_{5h})	a_1'	634.7		0.0	646.6	16.5
	a_1'	560.9		0.0	587.8	49.7
	e_1'	600.7		63.2	628.5	0.0
	e_1'	418.9		60.2	409.1	0.0
	e_1'	252.6		1.1	243.4	0.0
	e_2'	568.0		0.0	574.7	2.2
	e_2'	498.8		0.0	503.1	10.2
	a_2''	699.0		93.8	718.8	0.0
	a_2''	338.5		24.6	327.5	0.0
	e_1''	302.4		0.0	291.1	6.9
	e_2''	87.0		0.0	53.7	0.0
XeF_7^- (C_{2v})[f]	a_1	535.5		4.5	530.4	60.6
	a_1	524.9		395.0	497.5	5.7
	a_1	446.3		3.8	432.9	20.2
	a_1	331.4		0.2	321.2	2.0
	a_1	264.3		1.6	254.4	0.2
	a_1	204.3		0.0	203.1	2.7
	b_1	532.3		315.9	505.9	2.8
	b_1	315.9		0.0	313.9	2.0
	b_1	238.3		1.9	225.4	0.4
	b_1	202.1		0.5	182.1	1.2
	b_2	539.4		373.0	505.8	0.0
	b_2	437.4		6.9	418.7	12.6
	b_2	292.9		0.9	288.6	2.2
	b_2	249.7		1.5	237.7	0.1
	b_2	23.9		0.2	13.4	0.2
	a_2	449.2		0.0	442.0	26.3
	a_2	267.6		0.0	260.1	0.6
	a_2	30.9i		0.0	16.6	0.4
XeF_7^- (C_{3v})[f]	a_1	535.7		56.9	530.1	59.6
	a_1	531.1		351.7	500.2	4.9
	a_1	437.5		9.8	418.9	12.1
	a_1	279.2		1.5	272.0	1.6
	a_1	248.0		0.2	242.2	0.8
	a_2	231.5		0.0	225.9	0.0
	e	531.8		675.4	503.7	5.1
	e	447.8		4.6	437.1	46.7
	e	319.7		0.1	313.7	4.2
	e	263.9		2.1	254.1	1.4
	e	227.1		2.6	208.4	3.2
	e	25.2i		0.1	29.6i	0.9
XeF_7^- (D_{5h})[f]	a_1'	536.3		0.0	530.4	63.5
	a_1'	457.1		0.0	450.8	34.4
	e_1'	529.5		322.1	494.1	0.0
	e_1'	294.8		14.7	287.9	0.0
	e_1'	156.5		0.2	146.8	0.0
	e_2'	433.0		0.0	423.1	21.0
	e_2'	389.4		0.0	384.1	15.3
	a_2''	562.8		213.9	526.9	0.0
	a_2''	188.2		13.9	139.8	0.0
	e_1''	197.9		0.0	198.3	6.5
	e_2''	4.0		0.0	42.8i	0.0
XeF_8 (D_{4d})	a_1	577.4		0.0	554.3	66.3
	a_1	423.4		0.0	393.4	3.9
	b_1	228.2		0.0	205.3	0.0
	b_2	598.4		116.3	570.6	0.0
	b_2	411.1		65.8	393.4	0.0
	e_1	601.8		108.0	573.4	0.0
	e_1	428.1		78.4	400.0	0.0
	e_1	356.2		1.2	328.7	0.0
	e_2	543.8		0.0	512.1	2.9
	e_2	485.3		0.0	453.3	7.9
	e_2	126.1		0.0	110.4	0.5
	e_3	559.0		0.0	528.4	10.6
	e_3	426.1		0.0	395.8	6.3

[a] Frequencies for XeF_3^+ and XeF_3^- calculated at the CCSD(T)/aVTZ level. The second set of frequencies for XeF_3 were calculated at the CCSD(T)/aVDZ level. [b] Experimental frequencies: XeF^+: ref 51. [c] Experimental frequencies: XeF_3^+: ref 49. [d] Experimental frequencies: XeF_3: ref 10. [e] Experimental frequencies: XeF_5^+: ref 50. [f] Experimental frequencies: XeF_7^-: ref 47. The experimental values are not given above because we cannot make direct comparative assignments. The experimental frequencies in cm^{-1} for the Cs^+ salt are: 560(IR), 552(R); 521(R); 500(R), 500(IR); 476(R); 450(IR), 445(R); 396(R), 392(IR), 386(R); 340(R), 266(R), 206(R).

at the same level.[11] For XeF_2, we also reoptimized the structure at the CCSD(T)/awCVTZ level, including the core electrons in the correlation treatment, and predict r(XeF) = 1.980 Å, so the core−valence correction shortens the Xe−F bond by 0.013 Å. The long r(XeF) distance of 2.322 Å in XeF_3 is calculated to be 0.330 Å longer than the equivalent distance in XeF_2. The lower level MP2 and DFT values are also in good agreement with our CCSD(T)/aVTZ geometry parameters.[10] At the DFT level,[10] the dissociation energy of the third Xe−F bond is predicted to be in the range of 8−20 kcal/mol. At the CCSD(T)/CBS_{CV} electronic energy level, XeF_3 is bound by only 0.3 kcal/mol with respect to XeF_2 + F. When the additional corrections are included (excluding the second order spin orbit correction for XeF_2), we predict that XeF_3 is actually unbound with respect to XeF_2 and F by 1.7 kcal/mol of which 0.5 kcal/mol is due to the difference

Table 2. Energy Differences in kcal/mol Between the C_s/C_{2v} Structures of XeF_3^-, the O_h/C_{3v} and O_h/C_{2v} Structures of XeF_6, and the C_{2v}/D_{5h} and C_{2v}/C_{3v} Structures of XeF_7^- [a]

	XeF_3^-	XeF_6		XeF_7^-	
basis set	$\Delta E(C_s-C_{2v})$	$\Delta E(O_h-C_{3v})$	$\Delta E(O_h-C_{2v})$	$\Delta E(C_{2v}-D_{5h})$	$\Delta E(C_{2v}-C_{3v})$
aVDZ	0.79	9.16	9.40	−0.79	0.12
aVTZ	1.16	2.44	3.42	0.40	0.07
aVQZ	1.28	0.96	1.99	0.55	0.08
CBS (DTQ)	1.35	0.19	1.24	0.62	0.09
awCVDZ	0.79	7.48	10.30	−0.34	0.08
awCVTZ	1.12	1.32	2.40	0.79	0.05
awCVQZ	1.23	0.33	1.46	1.02	0.03
CBS $(DTQ)_{CV}$	1.29	−0.12	1.10	1.14	0.02

[a] aV*n*Z values for XeF_6 from ref 11.

in the ZPE's favoring the $XeF_2 + F$ channel. Thus there is, at best, only a very weak complex between XeF_2 and an F atom, and the value of 1.7 kcal/mol is slightly outside our estimated error bars. The CCSD(T) result is consistent with the previous MP2 calculations,[10] which predicted that XeF_3 is unbound with respect to the $XeF_2 + F$ asymptote.

The expected symmetric T-shaped C_{2v} structure for XeF_3^- is derived from a pseudooctahedron with 3 lone pairs with Xe in the +2 oxidation state, an Xe−F in the plane, and two axial Xe−F groups. However, this symmetric structure distorts to a more stable structure with C_s symmetry, which is 1.3 kcal/mol lower in energy at the CCSD(T)/awCV*n*Z (CBS) level (Table 2). The distortion to C_s symmetry makes one of the nominal Xe−F axial bond lengths to be the shortest one, with the nominal Xe−F equatorial bond length being of intermediate value. This distortion was found by starting from the optimum MP2 structure, which is distorted.

XeF_5^+ has C_{4v} symmetry and is derived from an octahedron with one lone pair and the Xe in the +6 oxidation state. The calculated $r(Xe-F_a)$ distance is < 0.01 Å longer than the experimental value from the crystal structure, and the $r(Xe-F_e)$ distance is in good agreement with the average experimental value;[43] $r(Xe-F_a)$ is shorter than the $r(Xe-F_e)$ bond distance. The bonding in XeF_5^+ can be described as two 4e-3c bonds for the four equatorial fluorines and a covalent Xe−F for the axial F, consistent with the bond distances. When compared to the $r(Xe-F)$ distance in XeF_4, the $r(Xe-F_e)$ distances are considerably shorter by 0.102 Å. The change in oxidation state from +4 in XeF_4 to +6 in XeF_5^+, as well as the presence of the positive charge in the latter, is the major reason for the substantial decrease in the bond distance.

The neutral radical XeF_5 has C_{4v} symmetry and is predicted to be bound by 1.5 kcal/mol with respect to XeF_4 and an F atom at the CCSD(T)/CBS level including the additional corrections. The four equivalent XeF distances are predicted to be 1.935 Å at the CCSD(T)/aVTZ level, slightly shorter by 0.017 Å than the equivalent distance in XeF_4.[11] The long Xe−F bond is predicted to be 2.228 Å, shorter by 0.095 Å than the analogous distance in the XeF_3 radical.

We re-evaluated the energy differences between the O_h, C_{3v}, and C_{2v} structures of XeF_6 using scaled geometries as previously described, and find that the relative energies are very dependent on the quality of basis set as shown previously[11] (Table 2). The total energies used to obtain the energy differences are given as Supporting Information (Table SM-2). At the CCSD(T)/awCVDZ level, the C_{3v} structure is 7.48 kcal/mol higher in energy than the O_h structure, compared to the previous value for $\Delta E(O_h-C_{3v})$ = 9.16 kcal/mol.[11] $\Delta E(O_h-C_{3v})$ decreases by 6.16 kcal/mol at the CCSD(T)/awCVTZ level to 1.32 kcal/mol.[11] At the CCSD(T)/awCVQZ level, the C_{3v} structure is only 0.33 kcal/mol higher in energy than the O_h structure, compared to the previous value for the (O_h-C_{3v}) energy difference of 0.96 kcal/mol.[11] At the CCSD(T)/CBS level, the C_{3v} structure is lower in energy by 0.12 kcal/mol as compared to the O_h structure.[11] If the C_{3v} geometry were optimized, the C_{3v} structure would be even more stable than the O_h structure as the O_h geometry has been determined more accurately. At the CCSD(T)/awCVDZ level, the C_{2v} structure is 10.30 kcal/mol higher in energy than the O_h structure. Improvement of the basis set to the awCVTZ level leads to a decrease of 7.90 to 2.40 kcal/mol above the O_h structure. At the CCSD(T)/awCVQZ level, the C_{2v} structure is only 1.46 kcal/mol higher in energy than the O_h structure, and the energy difference reduces to 1.10 kcal/mol at the CCSD(T)/CBS (awCV*n*Z) level.

XeF_7^+ has D_{5h} symmetry as expected from the predicted and experimentally[44,45] observed structures for IF_7, which is isoelectronic to XeF_7^+. Given that the Xe oxidation state is now +8, $r(Xe-F_a)$ decreases in XeF_7^+ as compared to $r(Xe-F_a)$ in XeF_5^+. The increased steric crowding in the equatorial plane in XeF_7^+ leads to an increase in the $r(Xe-F_e)$ distance as compared to $r(Xe-F_e)$ in XeF_5^+. The $r(Xe-F_a)$ distance in XeF_7^+ is substantially shorter than the $r(Xe-F_a)$ distance in XeF_3^+, consistent with the change in oxidation state from +IV to +VIII. The bonding in XeF_7^+ can be described by a 4e-3c bond for the two axial atoms and a 10e-6c bond for the in plane atoms. Thus, the Xe−F axial bond length should be shorter than the Xe−F equatorial bond length.

XeF_7^- is derived from a Xe in the +VI oxidation state. It would have a D_{5h} geometry like IF_7 if the lone pair on

(43) Leary, K.; Templeton, D. H.; Zalkin, A.; Bartlett, N. *Inorg. Chem.* **1973**, *12*, 1726. The actual values upon which the average $Xe-F_e$ distance is based are as follows: 1.836 (7), 1.849 (7), 1.841 (7), 1.838 (8), 1.842 (7), 1.845 (8), 1.855 (8), and 1.835 (7) Å.

(44) Marx, R.; Mahjoub, R.; Seppelt, K.; Ibberson, R. M. *J. Chem. Phys.* **1994**, *101*, 585.

(45) Adams, W. J.; Thompson, H. B.; Bartell, L. S. *J. Chem. Phys.* **1970**, *53*, 4040.

Xe is not sterically active. If the lone pair is active, three structures are possible: a pseudo square antiprism with C_s symmetry, a monocapped trigonal prism with C_{2v} symmetry, or a monocapped octahedral structure with C_{3v} symmetry. The additional ligand may make it more difficult for the lone pair to be stereoactive, and we would expect XeF_7^- to be similar to XeF_6 with the structures with an active lone pair being of comparable energy to those with a stereo inactive lone pair. However, determining the lowest energy structure requires good treatments of the correlation energy (CCSD(T)) and large basis sets.

We evaluated the energy differences between the C_{2v}, C_{3v}, and D_{5h} structures of XeF_7^- (Table 2) with the geometries optimized at the CCSD(T)/aVTZ level, and find that the relative energies are very dependent on the quality of basis set as shown previously for XeF_6.[11] The lowest energy structure of XeF_7^- is predicted to be of C_{2v} symmetry, with the C_{3v} structure lying only 0.02 kcal/mol higher in energy at the CCSD(T)/awCV*n*Z (CBS) level. At the CCSD(T)/awCVDZ level, the D_{5h} structure is actually predicted to be lower in energy than the C_{2v} structure by 0.34 kcal/mol. Only with an increase in the quality of the basis set does the C_{2v} structure become lower in energy, and at the CCSD(T)/awCVTZ level, the D_{5h} structure is predicted to be higher in energy by 0.79 kcal/mol. At the CCSD(T)/awCV*n*Z (CBS) level, the C_{2v} structure is lower in energy than the D_{5h} structure by 1.14 kcal/mol. (At the only level which we could compute the pseudo square antiprism with C_s symmetry geometry and frequencies (MP2/awCVDZ), the structure is very close to a D_{5h} geometry (minor deviations in the $\angle F_a-Xe-F_a$ and $\angle F_e-Xe-F_e$ from the ideal values of 180° and 72° and small differences for the bond distances.) We were only able to calculate the vibrational frequencies at the MP2/aVTZ level. At this level or at the B3LYP level, the lowest energy vibrational mode is approximately zero or is a small imaginary frequency for all three structures. This is consistent with a highly fluxional molecule.

Seppelt and co-workers[46] reported a crystal structure for $Cs^+XeF_7^-$ with the XeF_7^- having C_{3v} symmetry. Our calculated CCSD(T)/aVTZ geometry parameters are in reasonable agreement with the values from the crystal structure. The axial (capping) Xe−F bond distance is predicted to be shorter than the crystal structure value by 0.06 Å. The three Xe−F bonds in the capped-triangle are predicted to be longer by 0.07 Å. The three Xe−F bonds in the triangle furthest from the cap are essentially the same as the experimental value. The differences in the axial Xe−F and capped-triangle Xe−F distances between theory and experiment are consistent with an interaction of the capping F with the Cs^+ cation pulling it away from the Xe and enabling the capped-triangle Xe−F bonds to shorten in the crystal. The crystal structure of NO_2^+ with $Xe_2F_{13}^-$ has been reported,[46] and the XeF_7^- moiety within the $Xe_2F_{13}^-$ anion has C_{2v} symmetry. This structure of XeF_7^-, which closely interacts with an XeF_6, is quite different and is probably not a good experimental model for the isolated C_{2v} structure of XeF_7^-. Christe and co-workers[47] have published the vibrational spectra of XeF_7^- complexes with Cs^+ and NF_4^+ and find several common Raman and IR bands, suggesting that the lone pair is sterically active and XeF_7^- having either C_{3v} or C_{2v} symmetry. In D_{5h} symmetry, the Raman and IR bands should be mutually exclusive. However, the calculated vibrational spectra (see below) did not allow for a distinction between the C_{3v} and the C_{2v} structures. This is consistent with XeF_7^- being highly fluxional as the C_{2v}, C_{3v}, and D_{5h} structures are all within less than 2 kcal/mol of each other.

The experimental structure for IF_8^-,[48] which is isoelectronic to XeF_8, is of D_{4d} symmetry (square antiprism), so we optimized XeF_8 in the same type of structure with D_{4d} symmetry. The Xe−F bond distance in XeF_8 is 0.044 Å longer than the Xe−F bond distances in XeF_6 (O_h) at the CCSD(T)/aVTZ level.[11] Upon oxidative addition of F_2 to XeF_2, there are sequential decreases in the r(XeF) bond distances of XeF_4 and XeF_6 (O_h) of 0.039 and 0.010 Å at the CCSD(T)/aVTZ level, respectively.[11] In XeF_8, the ∠FXeF bond angle between neighboring fluorine atoms within one hemisphere is calculated to be 73.0°, and the ∠FXeF bond angle between fluorine atoms of separate square planes is calculated to be 78.0° at the CCSD(T)/aVTZ level.

Vibrational Frequencies. The calculated frequencies (Table 1) can be compared with experiment for XeF_3^+,[49] XeF_3,[10] XeF_5^+,[50] and XeF_7^- [47] in the solid state. For XeF^+, the MP2/aVTZ value for ω_e is 35 cm^{-1} higher than the value at the CCSD(T)/aVQZ level[11] and 59 cm^{-1} higher than the experimental value for $XeF^+Sb_2F_{11}^-$.[51] For XeF_3^+, the three Xe−F stretching frequencies calculated at the MP2 level are 26 to 40 cm^{-1} higher and the b_2 FXeF bending mode is 32 cm^{-1} lower than the experimental values, consistent with previous results. For XeF_3, the calculated CCSD(T) symmetric and antisymmetric Xe−F stretching modes of the XeF_2 moiety are 54 and 64 cm^{-1}, respectively, higher than the experimental Ar matrix values.[10] For XeF_2, the symmetric and antisymmetric stretches are predicted to be $\sigma_g^+ = 515.3$ cm^{-1} and $\sigma_u^+ = 566.8$ cm^{-1} at the CCSD(T)/aVDZ level respectively; the corresponding symmetric and antisymmetric Xe−F stretching modes of the XeF_2 moiety in XeF_3 are blue-shifted by ~66 cm^{-1}, which is consistent with the experimental results[10] where a blue-shift of ~20 cm^{-1} is observed in a solid Ar matrix and provides further indication of a weak complex of XeF_2 with F. For XeF_5^+, the calculated a_1 and b_2 stretching modes are 30 to 40 cm^{-1} higher, the e stretching mode is 72 cm^{-1} higher, and all of the bending modes are lower than the experimental values.[37]

For XeF_7^-, the vibrational frequencies calculated for the C_{2v}, C_{3v}, and D_{5h} geometries can be compared with the experimental solid state frequencies. The observed spectra do not follow the rule of mutual exclusion for infrared (IR) and Raman (R) bands which one would expect for a point group with a center of symmetry, such as D_{5h}.[47] Therefore, the D_{5h} structure can be ruled out. The differences between the calculated C_{2v} and C_{3v}

(46) Ellern, A.; Mahjoub, A.-R.; Seppelt, K. *Angew. Chem., Int. Ed. Engl.* **1996**, *35*, 1123.
(47) Christe, K. O.; Wilson, W. W. *Inorg. Chem.* **1982**, *21*, 4113.
(48) Mahjoub, A. R.; Seppelt, K. *Angew. Chem., Int. Ed. Engl.* **1991**, *30*, 876.
(49) McKee, D. E.; Adams, C. J.; Bartlett, N. *Inorg. Chem.* **1973**, *12*, 1722.
(50) Christe, K. O.; Curtis, E. C.; Wilson, R. D. *J. Inorg. Nucl. Chem.* **1976**, *28*, 159.
(51) Sladky, F. O.; Bulliner, P. A.; Bartlett, N. *J. Chem. Soc. A* **1969**, 2179.

Table 3. CCSD(T) Atomization and Reaction Energies in kcal/mol[a]

molecule	CBS[b]	ΔE_{ZPE}[c]	ΔE_{SR}[d]	ΔE_{SO}[e]	$\sum D_0(0K)$[f]
$XeF^+ + e^- \rightarrow Xe + F\cdot$	−237.39	0.92	−0.07	−0.39(2.09)	−236.68
$XeF^- \rightarrow Xe + F\cdot + e^-$	85.45	0.18	−0.19	−0.39	84.69
$XeF_2 \rightarrow Xe + 2F\cdot$	63.79	2.16	−0.32	−0.78(0.97)	61.50
$XeF_3^+ + e^- \rightarrow Xe + 3F\cdot$	−179.45	3.86	−0.49	−1.17	−184.96
$XeF_3 \rightarrow Xe + 3F\cdot$	64.07	2.70	−0.43	−1.17	59.77
XeF_3^- (C_s) $\rightarrow Xe + 3F\cdot + e^-$	164.04	2.45	−0.58	−1.17	159.84
$XeF_4 \rightarrow Xe + 4F\cdot$	125.63	4.59	−0.63	−1.56	118.85
$XeF_5^+ + e^- \rightarrow Xe + 5F\cdot$	−99.44	7.84	−0.96	−1.95	−110.19
$XeF_5 \rightarrow Xe + 5F\cdot$	127.97	4.72	−0.91	−1.95	120.38
$XeF_5^- \rightarrow Xe + 5F + e^-$	265.15	5.84	−1.01	−1.95	256.35
XeF_6 (O_h) $\rightarrow Xe + 6F\cdot$	182.33	6.88	−1.27	−2.34	171.85
$XeF_7^+ + e^- \rightarrow Xe + 7F\cdot$	−82.27	10.99	−1.37	−2.73	−97.36
XeF_7^- (C_{2v}) $\rightarrow Xe + 7F\cdot + e^-$	333.65	8.37	−1.68	−2.73	321.04
$XeF_8 \rightarrow Xe + 8F\cdot$	204.72	13.28	−1.82	−3.12	186.50
$KrF_3^- \rightarrow Kr + 3F\cdot + e^-$	121.62	2.54	−0.25	−1.17	117.66[g]
$KrF_5^- \rightarrow Kr + 5F\cdot + e^-$	154.69	5.48	−0.16	−1.95	147.10[g]
$KrF_7^- \rightarrow Kr + 7F\cdot + e^-$	169.35	8.06	0.20	−2.73	156.87[g]

[a] The radical energies were calculated with the R/UCCSD(T) method. [b] Extrapolated by using eq 1 with the awCVDZ, awCVTZ, and awCVQZ basis sets except for Kr where the aVDZ, aVTZ, and aVQZ basis sets (aug-cc-pV*n*Z-PP on Kr and aug-cc-pV*n*Z on F) were used. [c] The zero point energies were taken as 0.5, the sum of the appropriate calculated harmonic frequencies. See text. [d] The scalar relativistic correction is based on a CISD(FC)/VTZ MVD calculation and is expressed relative to the CISD result without the MVD correction, i.e., including the existing relativistic effects on Xe resulting from the use of a relativistic effective core potential. [e] Correction due to the incorrect treatment of the atomic asymptotes as an average of spin multiplets. Values are based on C. Moore's Tables, ref 28. [f] The theoretical value of ΔD_0 (0 K) was computed with the CBS estimates. [g] $\sum D_0$ (0 K) includes a ΔE_{CV} correction of −0.24, −0.93, and −1.89 kcal/mol for KrF_3^-, KrF_5^-, and KrF_7^-, respectively, obtained with the wCVTZ (F) and wCVTZ-PP (Kr) basis sets at the optimized CCSD(T) geometries.

Table 4. Calculated Heats of Formation (kcal/mol)[a]

	ΔH_f (DTQ)$_{CV}$		ΔH_f (DTQ)	
molecule	theory (0 K)	theory (298 K)	theory (0 K)	theory (298 K)
XeF^+ ($C_{\infty v}$)	255.1	254.7	255.8[b]	255.4[b]
	253.2 ± 3.7[c]			
XeF^- ($C_{\infty v}$)	−66.2	−66.7	−66.3[b]	−66.8[b]
XeF_2 ($D_{\infty h}$)	−24.6	−25.6	−23.3[b]	−23.9[b]
	−25.3,[d] *−28.0 ± 0.5*[e]			
XeF_3^+ (C_{2v})	240.4	239.3	240.1	238.9
XeF_3 (C_{2v})	−4.4	−4.6	−4.7	−5.0
XeF_3^- (C_s)	−104.4	−104.9	−104.7	−105.2
XeF_4 (D_{4h})	−45.0	−46.0	−42.5[b]	−43.5[b]
	−50.2, [d] *−57.7 ± 2*[e]			
XeF_5^+ (C_{4v})	202.5	200.5	204.2	202.2
XeF_5 (C_{4v})	−28.0	−28.4	−27.5	−27.9
XeF_5^- (D_{5h})	−164.0	−166.3	−160.6[b]	−162.9[b]
XeF_6 (O_h)	−61.0	−63.4	−55.9[b]	−58.3[b]
	−68.1, [d] *−(90$_{-3}^{+8}$)*[e]			
XeF_7^+ (D_{5h})	226.7	223.9	228.7	225.9
XeF_7^- (C_{2v})	−191.7	−193.3	−192.4	−194.6
XeF_8 (D_{4d})	−38.7	−42.4	−37.3	−40.9
KrF_3^- (C_s)			−62.0	−62.5
KrF_5^- (D_{5h})			−53.8	−55.0
KrF_7^- (D_{5h})			−27.6	−27.7

[a] Experimental values are given in italics. ΔH_f (DTQ)$_{CV}$ is based on CBS extrapolation of the awCVDZ, awCVTZ, and awCVQZ energies using eq 1, and for ΔH_f (DTQ), the extrapolation uses the aVDZ, aVTZ, and aVQZ energies (aug-cc-pV*n*Z-PP on Kr and Xe and aug-cc-pV*n*Z on F). [b] Ref 11. [c] Calculated from the collision induced dissociation energy for $XeF^+ \rightarrow Xe^+ + F$ (1.95 ± 0.16 eV = 45.0 ± 3.7 kcal/mol) with the heat of formation of Xe^+ (279.72 kcal/mol) and the heat of formation of F.[11,30,58] [d] Ref 53. [e] Re 54.

spectra are small, and both give a fair fit with the observed spectra.[34] Therefore, it is not possible to distinguish between these two point groups based on the experimental vibrational spectra.

Heats of Formation. The energetic components for predicting the total molecular dissociation energies are given in Table 3. The scalar relativistic corrections are all negative, except for KrF_7^- (+0.20 kcal/mol), and not large with values that range from −0.07 to −1.82 kcal/mol (the limits are for XeF^+ and XeF_8, respectively). We estimate that the error bars for the calculated heats of formation are ±1.0 kcal/mol considering errors in the energy extrapolation, frequencies, and other electronic energy components for most compounds. An estimate of the potential for significant multireference character in the wave function can be obtained from the T_1 diagnostic[52] for the CCSD calculation. The values for the T_1 diagnostics are calculated at the CCSD(T)/aVQZ level and given as Supporting Information (Table SM-4). The T_1 diagnostics are < 0.03 showing that the wave function is dominated by a single configuration.

The calculated heats of formation at 0 and 298 K are presented in Table 4. We have also recalculated the heats of formation of the neutral XeF_x compounds ($x = 2, 4, 6$) as well as XeF^- and XeF_5^- based on the CBS extrapolation of the awCV*n*Z (n = D, T, Q) electronic energies. Our new value for the heat of formation of XeF^- is essentially the same as our previous value.[11] Our new value for the heat of formation of XeF_2 is 1.3 kcal/mol more stable than our previously reported value of −23.3 kcal/mol at 0 K,[11] and is now in excellent agreement with the reported experimental value of −25.3 kcal/mol at 0 K, differing by only 0.7 kcal/mol. Our new calculated value for XeF_4 is more stable by 2.5 kcal/mol than our previously calculated value of −42.5 kcal/mol at 0 K,[11] but still differs by 5.2 kcal/mol from the most positive reported experimental value of −50.2 kcal/mol at 0 K. This experimental value was obtained from classical thermodynamic equilibrium measurements ($Xe + F_2 \leftrightarrow XeF_2$, $Xe + 2F_2 \leftrightarrow XeF_4$, $Xe + 3F_2 \leftrightarrow XeF_6$) at elevated temperatures in combination with predicted entropies.[53]

(52) Lee, T. J.; Taylor, P. R. *Int. J. Quantum Chem. Symp.* **1989**, *23*, 199.
(53) Weinstock, B.; Weaver, E. E.; Knop, C. P. *Inorg. Chem.* **1966**, *5*, 2189.

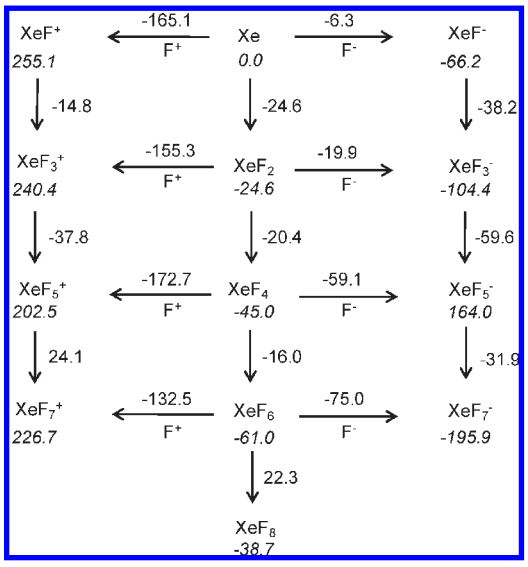

Figure 2. Heats of formation and reaction enthalpies for the addition of an F^+ or F^- ion and for the addition of F_2 at 0 K to Xe and its fluorides. All values in kcal/mol. Values in italics are heats of formation at 0 K. Vertical arrows correspond to the addition of F_2 to XeF_x to form XeF_{x+2} in terms of the cation, neutral, and anion. Horizontal arrows to the left correspond to F^+ affinity of XeF_x to form XeF_{x+1}^+ species. Horizontal arrows to the right correspond to the F^- affinity of XeF_x to form XeF_{x+1}^- species. The heats of formation of F^+ and F^- are 420.2 and −59.96 kcal/mol, respectively.[30] For all species, the DTQ_{CV} values of Table 4 were used.

The heats of formation of XeF_2, XeF_4, and XeF_6 have also been obtained from photoionization (PI) experiments,[54] based on extrapolated appearance potential measurements for reactions such as $XeF_2 + h\nu \rightarrow Xe^+ + F^- + F$ and $XeF_2 + h\nu \rightarrow XeF^+ + F^-$. The PI value of -57.7 ± 2 kcal/mol is substantially more negative than our value and appears to have a large error. The effect of extrapolating the CV correction for $\Delta H_f(XeF_6)$ gives an effect of 5.1 kcal/mol at 0 K, further stabilizing XeF_6 as compared to the single basis set CV value; our best calculated value still differs by 7.1 kcal/mol from the equilibrium experimental value of −68.1 kcal/mol at 0 K. The error in the PI value is much larger than for XeF_4. Because of the difficulty in obtaining the structure for XeF_6, we estimate the error in the heat of formation could be as large as ±2.0 kcal/mol. Clearly the PI values[54] are far too negative, overstabilizing the XeF_x compounds. Our calculated values suggest that there are issues with the equilibrium thermodynamic values of XeF_4 and XeF_6,[53] and we note that it is difficult to obtain high accuracy experimental thermodynamic data for such reactive species. Our new value for the heat of formation of XeF_5^- is predicted to be more stable by 3.4 kcal/mol at 0 K than our previous value.[11]

F^+ and F^- Affinities. The calculated heats of formation at 0 K allow us to calculate the F^+ (FPA) and F^- (FA) affinities of the corresponding neutrals at 0 K (Figure 2), given as $-\Delta H$ for the following respective reactions:

$$XeF_x + F^+ \rightarrow XeF_{x+1}^+ \quad (3)$$

$$XeF_x + F^- \rightarrow XeF_{x+1}^- \quad (4)$$

The actual enthalpies without the change in sign are reported in Figure 2. The F^+ affinity of XeF_2 is calculated to be 155.3 kcal/mol (6.73 eV), and the previously reported local density functional theory (DFT) value of 152.4 kcal/mol differs by only 3 kcal/mol.[14] The local DFT calculations were done with numerical basis sets[55] and the von Barth and Hedin fit[56] of the exchange-correlation energy of the uniform electron gas. The F^+ affinity of XeF_4 is the highest calculated for the neutral molecules and is predicted to be 172.7 kcal/mol (7.49 eV), differing by 14 kcal/mol from the previously reported local DFT value of 158.9 kcal/mol.[14] Our present value for the FPA(Xe) of 165.1 kcal/mol (7.16 eV) is in excellent agreement with the previously reported CCSD(T)/CBS (aV*n*Z) value of 163.6 kcal/mol (7.09 eV)[11] and the local DFT value of 164.8 kcal/mol (7.15 eV).[14] The F^+ affinity of XeF_6 is calculated to be the lowest of the neutrals at 132.5 kcal/mol (5.75 eV), consistent with the largest steric interactions. Our more accurately calculated value differs by 16 kcal/mol from the previously reported local DFT value of 116.7 kcal/mol.[14] Our present value for the FPA of XeF_6 is 33 kcal/mol less than that of Xe. These values are consistent with the trend predicted with lower level local DFT calculations[14] for the FPAs of Xe, XeF_2, XeF_4, and XeF_6, where the FPA of the fluorides are predicted to be below that of the atom. As shown in Figure 2, the F^+ affinities increase with increasing oxidation state of xenon, except for XeF_5^+. The unexpectedly low value for XeF_5^+ might be explained by its energetically favored pseudo-octahedral structure.

The fluoride affinities increase from Xe to XeF_6 as the formal oxidation state of the Xe becomes more positive (Figure 2). The effective oxidation state of the Xe is more important than any steric crowding in the molecule.

Sequential Addition of F_2. The various reactions possible for the Xe compounds are also summarized in Figure 2. We focus on the sequential addition of F_2 to the neutral, cationic, and anionic xenon fluorides. For the neutrals, the exothermicity of the addition of F_2 decreases as more F_2's are added to Xe. Whereas the sequential additions of F_2 to Xe, XeF_2, and XeF_4 are exothermic, the addition of F_2 to XeF_6 is an endothermic process. Thus, XeF_8 is thermodynamically unstable with respect to loss of F_2, but this F_2 elimination must have a significant activation energy barrier because XeF_8 is predicted to be vibrationally stable with no imaginary frequency. The decreasing heats of reaction for the sequential addition of F_2 to Xe, XeF_2, XeF_4, and XeF_6 are consistent with the increasing steric crowding of the F atoms around the central Xe atom. The current values of 24.6, 20.4, and 16.1 kcal/mol at 0 K, respectively, for sequential addition of F_2 to Xe, XeF_2, and XeF_4, are in good agreement with our previously reported values of 23.3, 19.2, and 13.4 kcal/mol.[11]

The average Xe−F bond dissociation energies (BDEs) in XeF_2, XeF_4, and XeF_6 decrease slightly with increasing oxidation state of Xe from 30.7 to 29.7 to 28.6 kcal/mol at 0 K, respectively, in good agreement with the previously reported values.[11] The average Xe−F bond energy of

(54) Berkowitz, J.; Chupka, W. A.; Guyon, P. M.; Holloway, J. H.; Spohr, R. *J. Phys. Chem.* **1971**, *75*, 1461.
(55) Delley, B. *J. Chem. Phys.* **1990**, *92*, 508.
(56) von Barth, U.; Hedin, L. *Physica C* **1972**, *5*, 1629.

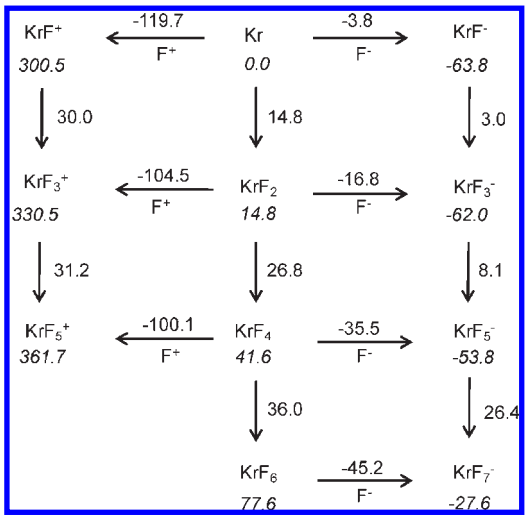

Figure 3. Heats of formation and reaction enthalpies for the addition of an F^+ or F^- ion and for the addition of F_2 at 0 K to Kr and its fluorides. All values in kcal/mol. Values in italics are heats of formation at 0 K. Vertical arrows correspond to the addition of F_2 to KrF_x to form KrF_{x+2} in terms of the cation, neutral, and anion. Horizontal arrows to the left correspond to F^+ affinity of KrF_x to form KrF_{x+1}^+ species. Horizontal arrows to the right correspond to the F^- affinity of KrF_x to form KrF_{x+1}^- species. The heats of formation of F^+ and F^- are 420.2 and −59.96 kcal/mol, respectively.[30] For all species, the DTQ values of Table 4 or ref 12 were used.

XeF_8 is calculated to be 23.3 kcal/mol. Therefore, the average bond energies decrease by 7.4 kcal/mol (~32% of the average bond energy for XeF_8) from XeF_2 to XeF_8.

The heats of formation of XeF_5 and XeF_3 provide us with more insights into the bonding in XeF_4 and XeF_6. The loss of the first F atom from XeF_6 to form XeF_5 is endothermic by 51.5 kcal/mol at 0 K and the loss of F from XeF_5 to form XeF_4 is endothermic by 1.5 kcal/mol, so most of the energy is lost in breaking the first Xe−F bond in XeF_6. We can calculate the first BDE in XeF_4 at 0 K as 59.1 kcal/mol. This is actually larger than the energy difference between XeF_4 and XeF_2 + 2F of 57.4 kcal/mol as XeF_3 is predicted to be unbound with respect to XeF_2 + F by 1.7 kcal/mol. The Xe−F BDE of XeF has been determined in a spectroscopic experiment to be 3.0 kcal/mol.[57,58] Use of this value gives a first BDE in XeF_2 of 58.6 kcal/mol at 0 K. Thus, the first Xe−F BDE increases from XeF_6 to XeF_4 by 7.6 kcal/mol and decreases slightly from XeF_4 to XeF_2 by 0.5 kcal/mol. Essentially all of the bond energy for the first two bonds is in the first Xe−F bond in XeF_2, XeF_4, and XeF_6.

Addition of F_2 to XeF^+ and XeF_3^+ is exothermic, and the exothermicity increases from XeF_3^+ to XeF_5^+. The increase in exothermicity from XeF_3^+ to XeF_5^+ is consistent with the structural change from the less favorable trigonal bipyramid structure in XeF_3^+ to the energetically favored octahedron in XeF_5^+. Again, the last addition of F_2 to XeF_5^+ is predicted to be endothermic, so steric crowding becomes important in XeF_7^+; again, XeF_7^+ is predicted to be a vibrationally stable structure.

Just as found for the cations, addition of F_2 to XeF^- and XeF_3^- is exothermic and the exothermicity increases from formation of XeF_3^- to that of XeF_5^-. In contrast to the cations, the addition of F_2 to XeF_5^- remains an exothermic process, but the exothermicity is about one-half of that of the addition of F_2 to XeF_3^-. The addition of F_2 to the anions is overall substantially more exothermic than the addition of F_2 to the cations. This is expected because for the same oxidation state cations are stronger oxidizers than the anions and, therefore, are more difficult to oxidize. The decrease in exothermicity on going from XeF_5^- to XeF_7^- can again be attributed to increased steric crowding.

Krypton Fluorides. We have previously reported values for the analogous krypton fluorides.[12] We summarize these results together with a few new, additional heats of formation in Figure 3. As discussed previously, the sequential addition of F_2 to the Kr fluorides starting with Kr is an endothermic process and the endothermicity increases with increasing fluorination. Addition of F_2 to KrF^+ and KrF_3^+ are also endothermic processes, but the endothermicity is essentially the same. Sequential addition of F_2 to the anions is also an endothermic process starting with KrF^-, and the reaction endothermicity increases with increasing number of fluorines. As expected from the Xe anion results, the reactions are less endothermic than for the neutral fluorides.

Conclusions

We have predicted the heats of formation for XeF_3^+, XeF_3, XeF_3^-, XeF_5^+, XeF_5, XeF_7^+, XeF_7^-, and XeF_8 at the CCSD(T)/CBS level plus additional corrections. Unlike the previously studied XeF_2, XeF_4, and XeF_6, XeF_8 is predicted to be thermodynamically unstable with respect to loss of F_2, and the reaction is calculated to be exothermic by 22.3 kcal/mol at 0 K. For the cations, XeF_7^+ is predicted to be thermodynamically unstable by 24.1 kcal/mol with respect to loss of F_2 to form XeF_5^+. XeF_3^+ and XeF_5^+ are predicted to be thermodynamically stable by 14.8 and 37.8 kcal/mol with respect to loss of F_2 to form XeF^+ and XeF_3^+, respectively. The F^+ affinities of Xe, XeF_2, XeF_4, and XeF_6 are predicted to be 165.1, 155.3, 172.7, and 132.5 kcal/mol, respectively, at 0 K, making XeF_5^+ the weakest oxidizer within this series of cations. The F^- affinities of Xe, XeF_2, XeF_4, and XeF_6 are predicted to be 6.3, 19.9, 59.1, and 75.0 kcal/mol, respectively, at 0 K. Thus, the Lewis acidity of the neutral xenon fluorides increases with increasing oxidation state of Xe and increasing number of fluorine ligands. Because of the high maximum coordination number of Xe toward fluorine, the steric influences are relatively minor.

Our results also provide evidence that, for XeF6 and XeF7$^-$, the structures with a sterically active free valence electron pair on Xe are favored over those with an inactive pair, although the energy differences are small, only about 2 kcal/mol. Thus, these highly coordinated xenon fluorides are expected to be very fluxional molecules which is consistent with the experimental structural and spectroscopic observations.

Acknowledgment. This research was supported, in part, by the U.S. Department of Energy, Office of Basic Energy Research, Chemical Sciences, in the catalysis program. This research was performed, in part, using the Molecular Science Computing Facility (MSCF) in the William R. Wiley Environmental Molecular Sciences Laboratory at

(57) Tellinghuisen, P. C.; Tellinghuisen, J.; Coxon, J. A.; Velazco, J. E.; Setser, D. W. *J. Chem. Phys.* **1978**, *68*, 5187.
(58) Krouse, I. H.; Wenthold, P. G. *Inorg. Chem.* **2003**, *42*, 4293.

the Pacific Northwest National Laboratory. The MSCF is a national user facility funded by the Office of Biological and Environmental Research in the U.S. Department of Energy. The Pacific Northwest National Laboratory is a multiprogram national laboratory operated by Battelle Memorial Institute. K.O.C. is grateful to the Air Force Office of Scientific Research, the Office of Naval Research, the National Science Foundation, and the Defense Threat Reduction Agency for financial support. We thank Dr. Shenggang Li for help with some of the calculations.

Supporting Information Available: CCSD(T)/aV*n*Z total energies (E_h) as a function of basis set. CCSD(T)/awCV*n*Z total energies as a function of basis set. Calculated MP2 and CCSD(T) with the aVTZ basis set geometry parameters of the xenon fluoride molecules and their ions. T_1 diagnostics calculated at the CCSD(T)/aVQZ level. Calculated F^+ and F^- affinities. Calculated heats of reaction for loss of F_2 from the cationic, neutral and anionic xenon fluorides. Calculated CCSD(T)/aVTZ and experimental geometries of the krypton fluoride molecules and their ions. This material is available free of charge via the Internet at http://pubs.acs.org.